

Lattice vibrations and structural instability in Cesium near the cubic to tetragonal transition

Y. Kong and O. Jepsen

Max-Planck-Institut für Festkörperforschung, Heisenbergstr.1, D-70569 Stuttgart, Germany

Abstract

Under pressure cesium undergoes a transition from a high-pressure fcc phase (Cs-II) to a collapsed fcc phase (Cs-III) near 4.2GPa. At 4.4GPa there follows a transition to the tetragonal Cs-IV phase. In order to investigate the lattice vibrations in the fcc phase and seek a possible dynamical instability of the lattice, the phonon spectra of fcc-Cs at volumes near the III to IV transition are calculated using Savrasov's density functional linear-response LMTO method. Compared with quasiharmonic model calculations including non-central interatomic forces up to second neighbours, at the volume $V/V_0 = 0.44$ (V_0 is the experimental volume of bcc-Cs with $a_0=6.048\text{\AA}$), the linear-response calculations show soft intermediate wavelength $T_{[1\bar{1}0]}[\xi\xi 0]$ phonons. Similar softening is also observed for short wavelength $L[\xi\xi\xi]$ and $L[00\xi]$ phonons and intermediate wavelength $L[\xi\xi\xi]$ phonons. The Born-von Kármán analysis of dispersion curves indicates that the interplanar force constants exhibit oscillating behaviours against plane spacing n and the large softening of intermediate wavelength $T_{[1\bar{1}0]}[\xi\xi 0]$ phonons results from a negative (110)-interplanar force-constant $\Phi_{n=2}$. The calculated frequencies for high-symmetry K and W phonons and longitudinal X and L phonons decrease with volume compression. In particular, the frequencies of the $T_{[1\bar{1}0]}[\xi\xi 0]$ phonons with ξ around $\frac{1}{3}$ become imaginary and the fcc structure becomes dynamically unstable for volumes below $0.41V_0$. It is suggested that superstructures corresponding to the $\mathbf{q}\neq 0$ soft mode should be present as a precursor of tetragonal Cs-IV structure.

Keywords: Cesium, Phonon, Linear-response LMTO

1 Introduction

At ambient pressure cesium metal crystallises in a bcc structure with experimental lattice parameter $a_0 = 6.048\text{\AA}$ [1] at 0K, obtained from the high-temperature values by extrapolation. It is a simple s^1 metal with nearly free-electron character. Under pressure the s valence electrons are transferred to more localised d -like states[2], and cesium exhibits an interesting sequence of phase transitions[3-8]. At the pressure 2.3GPa a transition[3, 4] from bcc (Cs-I) to fcc (Cs-II) occurs with a small reduction of volume. Near 4.2GPa, the fcc Cs-II phase undergoes an isostructural transition[4] to a collapsed fcc phase Cs-III with a large volume reduction (9%). Then at 4.4GPa there follows a transition to the tetragonal Cs-IV phase[5] with a decrease of the coordination number from 12 in Cs-III to 8 in Cs-IV (strictly, 4 nearest neighbours at 3.349Å and 4 second-nearest neighbours at 3.542Å at 8 GPa). At higher pressures more complicated phases[6, 7, 8] appear.

Many detailed investigations have been devoted to the study of the phase transitions in cesium, both experimentally (see Ref.[7] and literature cited therein) and theoretically (see, e.g., Refs.[7-12]). The pressure-induced electronic $s \rightarrow d$ transition was believed to be the driving force for destabilising the highly symmetric low-pressure structures (bcc or fcc) with respect to lower symmetry structures. The transition III \rightarrow IV was attributed to the accelerated progress[5] of the $s \rightarrow d$ transition and the unusual decrease of the coordination number from Cs-III to Cs-IV has been interpreted in terms of directional bonding induced by the $s \rightarrow d$ transition[12, 15].

In general, the $s \rightarrow d$ electronic transition in cesium affects not only the static lattice properties by changing the electronic band structure but also the lattice vibrational properties by modifying the effective interatomic interactions. The structural behaviour of cesium may therefore be reflected in the phonon spectrum and it is therefore of interest to investigate the phononic behaviour with applied pressure. Glötzel and McMahan[11] suggested that an anomaly in the lattice vibrational contribution to the pressure is a possible mechanism for the isostructural II \rightarrow III transition. Recently, Christensen et al.[16] calculated phonon dispersions of fcc-Cs within the quasiharmonic approximation to study the thermal expansion coefficient of cesium and the isostructural transition. They found that below $V/V_0 = 0.375$ (V_0 is the experimental volume of bcc-Cs at ambient conditions) fcc-Cs becomes unstable due to softening of a transverse [110] phonon branch, which is characterised by a negative shear elastic constant C' . Very recently, Xie et al.[17] investigated the phonon instabilities of cesium using density-functional perturbation theory. Their calculations showed that the instability of the fcc cesium occurs at a volume of about $0.46V_0$, which is also driven by a

negative C' . However, it is not clear what happened with the phonons before the C' goes soft. Using the density functional linear-response LMTO method[18], we calculate the accurate phonon spectrum of fcc-Cs at the volumes near the III-IV transition to study the lattice vibrations in fcc-Cs and to seek a possible dynamical instability of fcc-Cs before C' becomes negative. According to our calculations, fcc-Cs becomes unstable at a volume slightly smaller than $V/V_0 = 0.41$. Soft $T_{[1\bar{1}0]}-\xi\xi 0$ phonons with $\xi \sim \frac{1}{3}$ are found to be responsible for the dynamical instability.

This paper is organised as follows. Some computational details concerning linear-response LMTO calculations are described in the next section. Section 3 presents the results obtained and some discussions. Firstly, the phonon dispersion curves for fcc-Cs at the volume $V/V_0 = 0.44$ are analysed in terms of force constants between atoms; then the phonon frequencies at various volumes are discussed in relation to the instability of the fcc structure. Several concluding remarks are given in the last section.

2 Computational Details

The density functional linear-response LMTO method[18] is used in the present study to calculate the phonon spectrum of fcc-Cs at the volumes around the Cs-III - Cs-IV transition. Phonon dispersion curves for a large number of simple and transition metals and a few compounds have been calculated by the linear-response LMTO method, and excellent agreement with experimental data were obtained.[18, 19] In the following we summarise some details of the calculations.

The dynamical matrix of fcc-Cs is calculated for a set of irreducible \mathbf{q} points in a (8,8,8)-reciprocal lattice grid (29 points per 1/48th part of the Brillouin Zone (BZ)). The (I,J,K) reciprocal-lattice grid is defined in the usual manner: $\mathbf{q}_{ijk} = (i/I)\mathbf{G}_1 + (j/J)\mathbf{G}_2 + (k/K)\mathbf{G}_3$, where \mathbf{G}_i are the primitive translations in reciprocal space. We chose the exchange-correlation potential of Vosko-Wilk-Nusair[20] plus the non-local generalised-gradient-approximation (GGA-96) correction[21]. Because this gave a better prediction of the equilibrium volume at ambient pressure and 0K which is only 4% smaller than the experimental zero-pressure volume at 0K. On the other hand, the local density approximation (LDA) gave a nearly 20% overbinding at ambient pressure. The calculated bcc to fcc transition pressure of 2.0GPa is in good agreement with the experimental value of 2.3GPa.[4]

In the calculations a $3\kappa - spd$ LMTO basis set is used with the one-center expansions inside the non-overlapping muffin-tin (MT) spheres performed up to $l_{max} = 6$. In the interstitial region, the s -, p - and d -basis functions are expanded in plane waves. The $5s$ semicore state is treated as valence state in a separate energy window. The induced charge densities

and screened potentials are represented inside the MT spheres by spherical harmonics up to $l_{max} = 6$ and by plane waves with a 148.4 Ry energy cutoff (9984 plane waves) in the interstitial region.

The \mathbf{k} -space integration is performed over a (16,16,16) grid (145 irreducible point) by means of the improved tetrahedron method[22], but the integration weights for these \mathbf{k} points are calculated from a denser (32,32,32) grid (897 points in the irreducible BZ). This results in a more accurate representation of the Fermi surface with a small number of \mathbf{k} points.

The phonons along the high-symmetry lines presented in the next section were calculated in a denser \mathbf{q} mesh which fit to the (16,16,16) \mathbf{k} -grid.

3 Results and Discussions

3.1 Phonon dispersions at $V/V_0 = 0.44$

Fig. 1 shows the calculated phonon dispersion curves along some high-symmetry directions for fcc-Cs at the volume $0.44V_0$, which is in the experimental volume range of the cubic to tetragonal phase transition. To the right the calculated phonon density of states (DOS) is plotted. The dash lines represent the fitted results by the Born-von Kármán model which is described in the next section. The calculated phonon frequencies at the high-symmetry zone-boundary (ZB) points L , X , K and W are listed in Table 1.

As observed in Fig. 1, the phonon frequencies of the $L[\xi\xi 0]$, $T[00\xi]$ and $T[\xi\xi\xi]$ branches exhibit rather normal dispersion while the $T[\xi\xi 0]$, $L[00\xi]$ and $L[\xi\xi\xi]$ dispersion curves show abnormal behaviour for intermediate and short wavelengths, which indicates long-range interactions between atoms. For the $L[\xi\xi\xi]$ phonon branch, small downwards anomaly is seen around $\xi = \frac{1}{4}$. Near the zone boundary, the $L[\xi\xi\xi]$ phonons have very little dispersion and the frequencies of the $L[00\xi]$ phonons are rather small compared to other fcc metals. The $T[\xi\xi 0]$ phonons have flat regions around $\xi = \frac{1}{3}$ and $\frac{3}{4}$ for the polarisation $[1\bar{1}0]$ (T_1) and $[001]$ (T_2), respectively. Since the phonon DOS in Fig. 1 was calculated at a coarse (8,8,8) grid, these abnormal behaviours are not clearly seen in the plotted DOS. Nevertheless, the sudden increase of DOS at the frequency just above 0.3 THz and the small sharp peak at the frequency near 1.6 THz indicate the presence of these anomalies.

In metals at equilibrium the long-range interatomic interactions are generally of little importance due to screening effect of the electrons. The lattice dynamical properties of metals can therefore be described well using a short-range force model. This, however, may not hold for cesium under high pressure. The pressure-induced electronic $s \rightarrow d$ transition causes the valence charge density of cesium to deviate from spherical symmetry with a consequent reduction in electronic screening and increased interactions between the atoms. To check

this, we calculate the phonon dispersion curves of fcc-Cs at the volume $V/V_0 = 0.44$ using a short-range force model within the quasiharmonic approximation. The dispersion relations are derived as in the usual harmonic approximation by considering non-central forces between atoms up to second neighbours and the four interatomic force constants involved in the dynamical matrices are obtained from the three calculated elastic constants[23] and the $T[100]$ zone boundary phonon frequency by expanding the elements of the dynamical matrix and finding its long-wavelength limit. The obtained dispersion curves are plotted in Fig. 1 by solid lines and the phonon frequencies at the zone boundaries are listed in Table 1. Note that the quasiharmonic results presented here are derived from a short-range force model, which does not exactly consider the electronic contribution to the dynamical matrix. The difference to the results from linear-response calculations may therefore reveal the effects of long-range interatomic interactions. It may be seen in Fig. 1 that the short-range non-central force model describes the $T[00\xi]$, $T[\xi\xi\xi]$ and $L[\xi\xi0]$ phonon dispersions quite well. However, the previously mentioned anomalies in the $L[00\xi]$, $L[\xi\xi\xi]$ and $T[\xi\xi0]$ dispersion curves calculated by the linear-response method are not reproduced and they may therefore be a consequence of long-range interactions.

In general, an abnormal behaviour of the phonon dispersion may be attributed to special properties of interatomic force constants. In the following subsection, we shall analyse the dispersion curves by using the Born-von Kármán model to find these special properties of the interactions between the atoms in fcc-Cs.

3.2 Born-von Kármán analysis of force constants

Since one of the motivations of the present work is to interpret the anomalies in the calculated phonon dispersion curves for fcc-Cs, it is necessary to use a model which can reproduce these anomalies. This could be achieved by a force-constant model based on the Born-von Kármán theory[24].

In the Born-von Kármán theory the frequencies $\nu(\mathbf{q})$ of the normal vibration modes for an fcc lattice with one atom per unit cell are given as the solutions of a 3×3 determinantal equation

$$|4\pi^2 M \nu^2(\mathbf{q}) \delta_{\alpha\beta} - C_{\alpha\beta}(\mathbf{q})| = 0, \quad (1)$$

where M is the mass of the atom and

$$C_{\alpha\beta}(\mathbf{q}) = \sum_{l'} \Phi_{\alpha\beta}(l, l') \exp[i\mathbf{q} \cdot \mathbf{R}(l, l')], \quad (2)$$

where $\Phi_{\alpha\beta}(l, l')$ is the $\alpha\beta$ component of the force constant matrix between the atoms in the l th and l' th cell. For the phonon modes along the three high-symmetry directions $[\xi\xi0]$, $[00\xi]$

and $[\xi\xi\xi]$, the $C_{\alpha\beta}$ matrices are diagonal and the solution of Eq.(1) leads to equations in ν^2 of the form

$$4\pi^2 M\nu^2 = \sum_n \Phi_n [1 - \cos(n\pi q/q_{max})], \quad (3)$$

where q_{max} is half the distance to the nearest reciprocal lattice point in the direction of \mathbf{q} , $q = |\mathbf{q}|$ and Φ_n is a sum of $\Phi_{\alpha\beta}(l, l')$ [25] for which the phase $\mathbf{q} \cdot \mathbf{R}(l, l')$ is a constant. Φ_n effectively represents a force between a plane of atoms and the planes of atoms normal to \mathbf{q} and n planes away. The summation includes N terms so that $\Phi_n = 0$ for $n > N$. Thus, a Fourier series analysis of the squares of the phonon frequencies will yield the interplanar force constants.

Accordingly, a least-squares Fourier fit are performed using Eq.(3) for the phonon dispersion curves of fcc-Cs at the volume $0.44V_0$ calculated from linear-response calculations. The fitted dispersion curves are plotted in Fig. 1 by the dashed lines. Within the accuracy of the calculated phonon frequencies, it is found that a satisfied fit can only be obtained by including at least four planes in the $[00\xi]$ branches, five planes in the $T[\xi\xi\xi]$ branch and even six planes in the $[\xi\xi0]$ and $L[\xi\xi\xi]$ branches. In Table 2 we list the fitted interplanar force constants Φ_n . Since four planes along the $[00\xi]$ direction correspond to interactions out to at least eighth neighbour atoms and five (six) planes along the $[\xi\xi\xi]$ ($[\xi\xi0]$) direction out to farther neighbours, the fitted results confirm the presence of long-range interactions between atoms in fcc-Cs. We plot the fitted Φ_n for the $T_{[1\bar{1}0]}[\xi\xi0]$ branch in Fig. 2a as a function of n , which effectively is the distance between planes of atoms. The Φ_n are observed to oscillate with the distance between planes, especially with a prominently negative $\Phi_{n=2}$. The values of ν^2 for the same phonon branch and the fitted curve with $N = 8$ are shown in Fig. 2b together with the individual contributions from the first five Fourier components. It is seen that the $n = 2$ planes produce a largely negative contribution to the frequencies of phonons, which partly cancels the dominant contribution from the $n = 1$ planes. Consequently, the soft intermediate-wavelength $T_{[1\bar{1}0]}[\xi\xi0]$ phonons result and a flat region of the dispersion curve is formed. A similar oscillating behaviour of the fitted Φ_n is seen in some of the other branches although they are less pronounced. The anomalies observed in the $T_{[001]}[\xi\xi0]$ and $L[\xi\xi\xi]$ dispersion curves can be associated with these oscillations. For the $L[00\xi]$ branch no oscillations in Φ_n is found. The very low phonon frequencies for long-wavelengths compared to the short-range model calculation may be attributed to the small value of $\Phi_{n=1}$.

The interplanar force constants can be used to derive interatomic force constants[25]. With a general force model, a linear least-square fitting analysis for the Φ_n in Table 2 only allows us to work out the interatomic force constants in fcc-Cs extending to the fourth neighbour. The truncation of the interactions with farther neighbours introduces large er-

rors in the fitting procedure and makes the fitted interatomic force constants less reliable. Nevertheless, in Table 3 we list the best fit values of the interatomic constants in fcc cesium.

3.3 Soft mode and lattice instability

The volume dependence of the high-symmetry zone-boundary L , X , K , and W phonons for fcc-Cs are presented in Fig. 3. From this the mode-Grüneisen parameter $\gamma_i = -(\partial \ln \nu_i / \partial \ln V)$ was derived and listed in Table 1. It may be seen that all the high-symmetry phonons except the transverse X and L phonons decrease with increasing pressure and consequently have negative mode-Grüneisen parameters, which may be an indication that the fcc structure is unstable under pressure.

In Fig. 4 we show the $T_{[1\bar{1}0]}[\xi\xi 0]$ phonon-dispersion curves of fcc-Cs for the volumes $V/V_0 = 0.37, 0.40, 0.41$, and 0.44 . At volumes between $V/V_0 = 0.41$ and 0.40 the phonon frequencies around $\xi = \frac{1}{3}$ become imaginary. However, the shear elastic constant C' does not become negative before the volume is reduced to $V/V_0 = 0.37$ where the entire phonon branch becomes unstable. Christensen et al.[16] and Xie et al.[17] inferred from their calculations that it is the pressure-induced negativity of C' which is the cause of the instability of the fcc phase. They however did not trace the development of the instability in details and it is clear from Fig. 4 that it is a $\mathbf{q} \neq 0$ $T_{[1\bar{1}0]}[\xi\xi 0]$ soft mode which drives the dynamical instability of the fcc phase close to $V/V_0 = 0.41$. As a consequence of the soft mode, superstructures should exist as a precursor to the tetragonal Cs-IV phase transition. It is interesting to note that the calculated transition volume $V/V_0 = 0.41 \sim 0.40$ is close to the volume where the fcc to tetragonal transition is observed[5]. In Fig. 5 we illustrate the displacement pattern of atoms in fcc-Cs corresponding a $T_{[1\bar{1}0]}[\frac{1}{4}\frac{1}{4}0]$ phonon mode and the resulting Cs superstructure. As seen from Fig. 5, a structural element of the displacement pattern is triangular prisms, which are also present in the Cs-IV structure, even though other possible soft modes as well as the coupling between phonons could be important.

Usually a soft phonon mode leads to a second-order or nearly first-order phase transition. Early experimental results[5] indicated that the Cs-III-Cs-IV transition is first-order in character with a 4.3% volume reduction. Therefore soft phonon modes should not be considered the unique driving force in the cesium III-IV phase transformation even though the soft mode leads to an instability in the fcc structure. The changes of the electronic properties under pressure, such as $s - d$ transition, must play an important role.

4 Conclusions

Using a density functional linear-response LMTO method, we have studied the phonon spectra of fcc cesium at volumes near the III-IV transition. Several anomalies in the dispersion curves have been found.

Within the Born-von Kármán theory of lattice dynamics, the observed anomalies in the calculated phonon dispersion curves for fcc-Cs at the volume $0.44V_0$ are connected with oscillating behaviours of the interplanar force constants against plane spacing n . In particular, a negative (110)-interplanar force-constant $\Phi_{n=2}$ is found to be responsible for soft intermediate-wavelength $T_{[1\bar{1}0]}[\xi\xi 0]$ phonons.

The frequencies of high-symmetry K and W and longitudinal X and L phonons decrease with volume compression and the consequent negative mode-Grüneisen parameters indicate an instability of fcc lattice under pressure. When the volume is below $0.41V_0$, the frequencies of the $T_{[1\bar{1}0]}[\xi\xi 0]$ phonons with ξ around $\frac{1}{3}$ becomes imaginary prior to the sign change of the shear elastic constant C' and the fcc lattice is thus dynamically unstable. It is suggested that superstructures corresponding to the $\mathbf{q}\neq 0$ $T_{[1\bar{1}0]}[\xi\xi 0]$ soft phonon should be present as a precursor of tetragonal Cs-IV structure. It was pointed out in Ref.[7] that the fcc structure of Cs-III could not be confirmed and that Cs-III appears to be a rather complicated structure. The present argument may stimulate further experimental study for reexamining the structure of Cs at the pressure near the Cs-II-Cs-III-Cs-IV transitions.

Acknowledgements

Y. Kong gratefully acknowledge helpful discussions and advice from Prof. O. K. Andersen, and we are grateful to Prof. K. Syassen for a critical reading of the manuscript.

References

- [1] M.S. Anderson, E.J. Gutman, J.R. Packard and C.A. Swenson, *J. Phys. Chem. Solids*, **30**, 1587 (1969).
- [2] R.M. Sternheimer, *Phys. Rev.* **78**, 235 (1950).
- [3] G.C. Kennedy, A. Jayaraman, and R.C. Newton, *Phys. Rev.* **126**, 1363 (1962).
- [4] H.T. Hall, L. Merrill, and J.D. Barnett, *Science* **146**, 1297 (1964).
- [5] K. Takemura, S. Minomura, and O. Shimomura, *Phys. Rev. Lett.* **49**, 1772 (1982).
- [6] K. Takemura, O. Shimomura, and H. Fujihisa, *Phys. Rev. Lett.* **66**, 2014 (1991).
- [7] U. Schwarz, K. Takamura, M. Hanfland, and K. Syassen, *Phys. Rev. Lett.* **81**, 2711(1998).
- [8] K. Takemura, N.E. Christensen, D.L. Novikov, K. Syassen, U. Schwarz, M. Hanfland, *Phys. Rev. B* **61**, 14399 (1998).
- [9] S.G. Louie and M.L. Cohen, *Phys. Rev. B* **10**, 3237 (1974).
- [10] A.K. McMahan, *Phys. Rev. B* **17**, 1521 (1978).
- [11] D. Glötzel and A.K. McMahan, *Phys. Rev. B* **20**, 3210 (1979).
- [12] A.K. McMahan, *Phys. Rev. B* **29**, 5982 (1984).
- [13] H.L. Skriver, *Phys. Rev. B* **31**, 1909 (1985).
- [14] S. Carlesì, A. Franchini, V. Bortolani, S. Martinelli, *Phys. Rev. B* **59**, 11716 (1999).
- [15] O.K. Andersen, N.E. Christensen, Z. Pawłowska and O. Jepsen (unpublished).
- [16] N.E. Christensen, D.J. Boers, J.L. van Velsen and D.L. Novikov, *Phys. Rev. B* **61**, R3764 (2000); *J. Phys.: Condens. Matter* **12**, 3293 (2000).
- [17] J. Xie, S.P. Chen, J.S. Tse, D.D. Klug, Z. Li and K. Uehara, L.G. Wang, *Phys. Rev. B* **62**, 3624 (2000).
- [18] S.Y. Savrasov, *Phys. Rev. Lett.* **69**, 2819 (1992); *Phys. Rev. B* **54**, 16470 (1996).
- [19] S.Y. Savrasov and D.Y. Savrasov, *Phys. Rev. B* **54**, 16487 (1996).
- [20] S.H. Vosko, L. Wilk and M. Nusair, *Can. J. Phys.* **58**, 1200 (1980).
- [21] J.P. Perdew, K. Burke and M. Ernzerhof, *Phys. Rev. Lett.* **77**, 3865 (1996).
- [22] P. Blöchl, O. Jepsen, and O.K. Andersen, *Phys. Rev. B* **49**, 16223 (1994).
- [23] The bulk modulus and shear moduli (C' , C_{44}) of fcc-Cs are calculated in a full-potential LMTO scheme. For the volume $0.44V_0$, $C_{11}=13.8\text{GPa}$, $C_{12}=11.0\text{GPa}$ and $C_{44}=8.1\text{GPa}$.
- [24] M. Born and K. Huang, in *Dynamical theory of crystal lattices* (Oxford University Press, New York, 1954).
- [25] B.N. Brockhause, T. Arase, G. Caglioti, K.R. Rao, and A.D.B. Woods, *Phys. Rev.*, **128**, 1099 (1962).

Tables

Table 1: Calculated phonon frequencies ν_i (THz) at the high-symmetry L , X , K and W points for fcc Cs at the volume $V/V_0 = 0.44$ and corresponding mode-Grüneisen parameters γ_i defined by $\gamma_i = -(\partial \ln \nu_i / \partial \ln V)$. Also listed in brackets are the frequencies from the short-range force model calculation.

		L	X	K	W
L -branch	ν_i	1.97 (2.13)	1.73 (2.10)	1.58 (1.65)	1.51
	γ_i	-0.95	-0.79	-0.80	-1.27
T_1 -branch	ν_i	0.82 (0.86)	1.36 (1.36)	0.95 (1.20)	1.23
	γ_i	0.71	0.49	-0.80	-1.60
T_2 -branch	ν_i	0.82 (0.86)	1.36 (1.36)	1.62 (1.93)	1.46
	γ_i	0.71	0.49	-0.93	-1.41

Table 2: Interplanar force constants Φ_n (up to $n = 6$) for fcc Cs at the volume $V/V_0 = 0.44$ in units of 10^{-3} Ry/bohr². The errors given are approximate errors for the fitted Φ_n . Note that a satisfactory fit for the $[00\xi]$ and $T[\xi\xi\xi]$ phonons is obtained with only four and five Fourier components, respectively.

	Φ_1	Φ_2	Φ_3	Φ_4	Φ_5	Φ_6	error
$T[00\xi]$	10.69	0.11	-0.24	-0.18	-	-	± 0.15
$L[00\xi]$	16.09	1.85	0.72	0.29	-	-	± 0.50
$T[\xi\xi\xi]$	4.11	0.49	-0.36	0.10	-0.05	-	± 0.02
$L[\xi\xi\xi]$	23.09	-0.86	-2.44	3.35	1.39	-2.78	± 0.50
$T_{[001]}[\xi\xi 0]$	16.32	3.56	-0.40	-1.06	0.80	-0.55	± 0.19
$T_{[1\bar{1}0]}[\xi\xi 0]$	8.51	-4.10	1.74	-0.42	0.21	0.09	± 0.11
$L[\xi\xi 0]$	8.88	14.52	1.29	-0.85	0.30	-0.29	± 0.12

Table 3: The best fit values of interatomic force-constants for fcc Cs at the volume $V/V_0 = 0.44$ in units of Ry/bohr². The force constant notation follows the definition of Brockhouse et al.[25].

Neighbour location	Force constants			Values (Ry/bohr ²)
First $\frac{a}{2}(1,1,0)$	α_1	γ_1	0	$\alpha_1 = 21.2 \times 10^{-4}$
	γ_1	α_1	0	$\beta_1 = -2.0 \times 10^{-4}$
	0	0	β_1	$\gamma_1 = 38.6 \times 10^{-4}$
Second $\frac{a}{2}(2,0,0)$	α_2	0	0	$\alpha_2 = -2.1 \times 10^{-4}$
	0	β_2	0	$\beta_2 = 5.8 \times 10^{-4}$
	0	0	β_2	
Third $\frac{a}{2}(2,1,1)$	α_3	δ_3	γ_3	$\alpha_3 = 3.6 \times 10^{-4}$
	δ_3	β_3	γ_3	$\beta_3 = -0.6 \times 10^{-4}$
	γ_3	γ_3	β_3	$\gamma_3 = 3.6 \times 10^{-4}$
Fourth $\frac{a}{2}(2,2,0)$				$\delta_3 = -0.4 \times 10^{-4}$
	α_4	γ_4	0	$\alpha_4 = -0.4 \times 10^{-4}$
	γ_4	α_4	0	$\beta_4 = 0.04 \times 10^{-4}$
	0	0	β_4	$\gamma_4 = -4.1 \times 10^{-4}$

Figure Captions

Figure 1: Calculated phonon-dispersion curves along three symmetry directions for fcc-Cs at the volume $V/V_0 = 0.44$. The squares are the calculated results using the density-functional linear-response method and the solid lines represent the results from a quasiharmonic calculation (see text). The dash lines are the fitted results by the Born-von Kármán model. Also plotted in the right panel is the phonon density of states derived from the linear-response calculations.

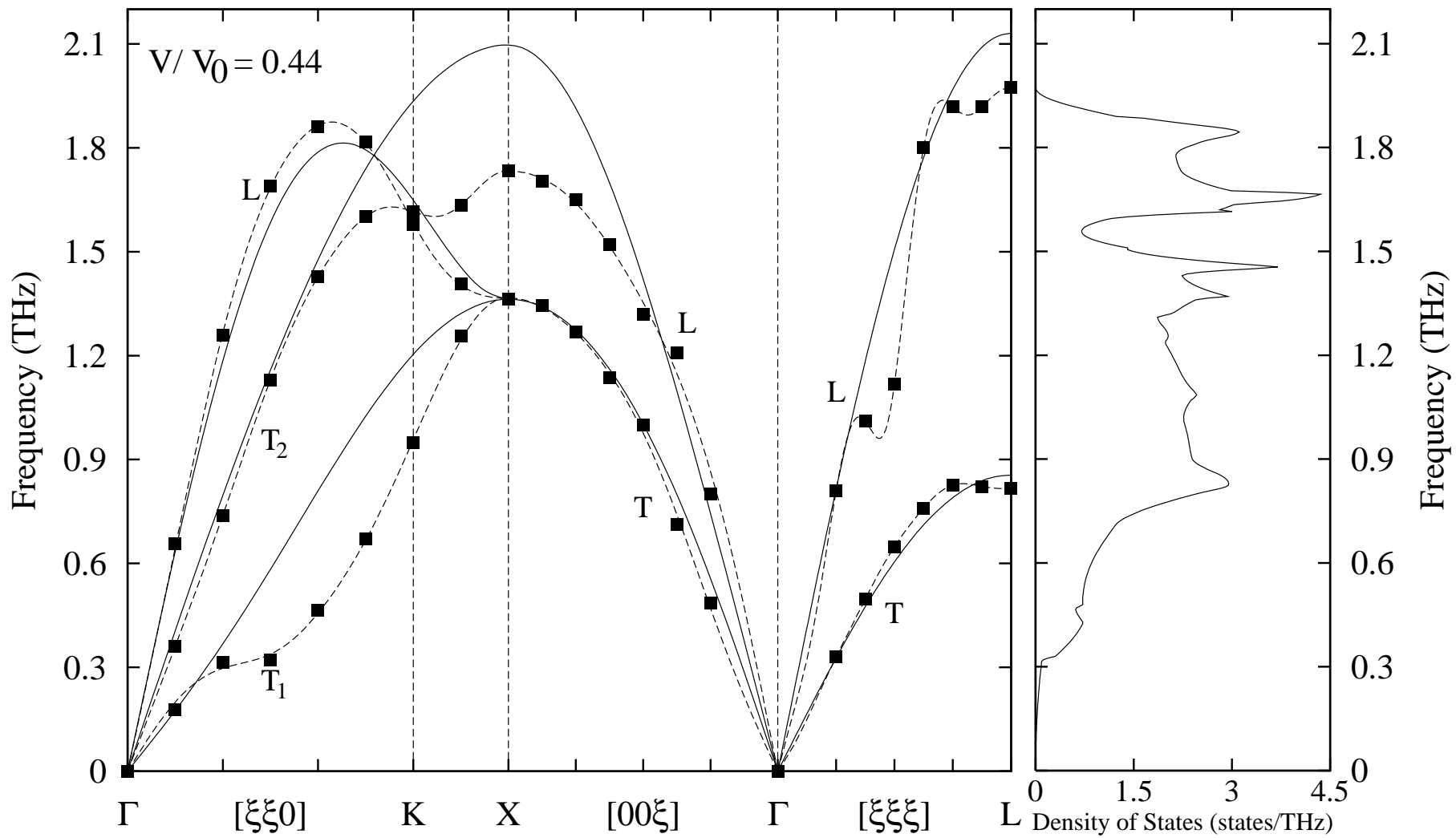
Figure 2: (a) The interplanar force constants (up to $n = 8$) for the $T_{[1\bar{1}0]}[\xi\xi 0]$ branch phonons of fcc-Cs at the volume $V/V_0 = 0.44$. A clear oscillating behaviour against the number of the plane (interplanar spacing) is seen. (b) Values of ν^2 for the same branch phonons plotted as a function of the reduced wave-vector. The fitted curve (solid line) with 8 planes are shown together with the contributions from the first five Fourier components.

Figure 3: Calculated phonon frequencies ν_i (THz) at the high-symmetry L , X , K and W points for fcc Cs as a function of the volume. (a) Longitudinal and (b) transverse branches.

Figure 4: Calculated $T_{[1\bar{1}0]}[\xi\xi 0]$ phonon-dispersion curve for fcc Cs at the volumes $V/V_0 = 0.37, 0.40, 0.41$, and 0.44 . The points are the calculated values and the lines result from the interpolation between points and are only a guide to the eye.

Figure 5: Schematic illustration of displacement pattern (left) of atoms in fcc-Cs corresponding a $T_{[1\bar{1}0]}[\frac{1}{4}\frac{1}{4}0]$ phonon and the resulting Cs superstructure (right). The lengths of solid arrows are proportional to the displacement of atoms and the dash arrows indicate the $[100]$, $[010]$ and $[110]$ directions of fcc lattice.

Fig. 1 of Y. Kong et al.



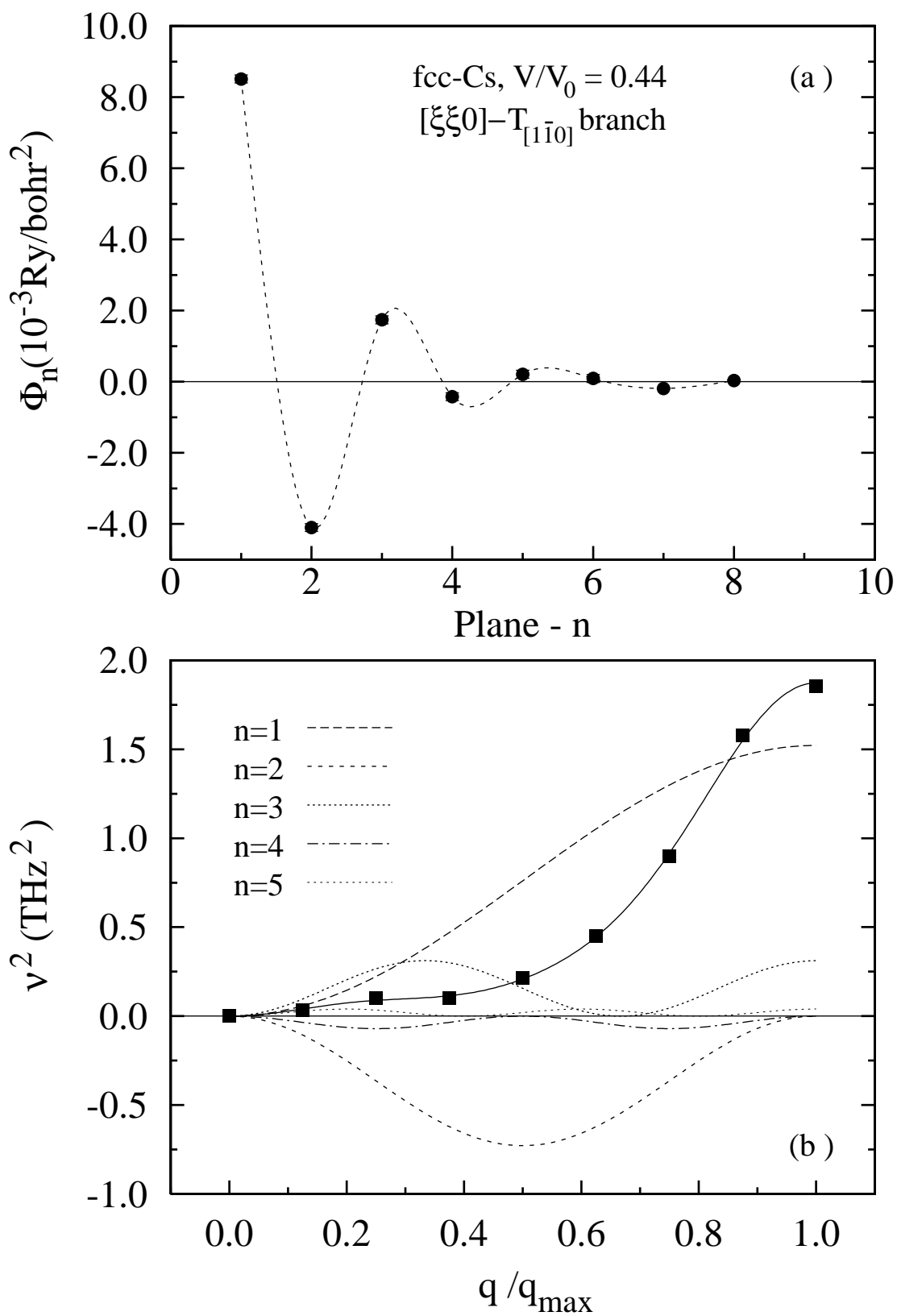
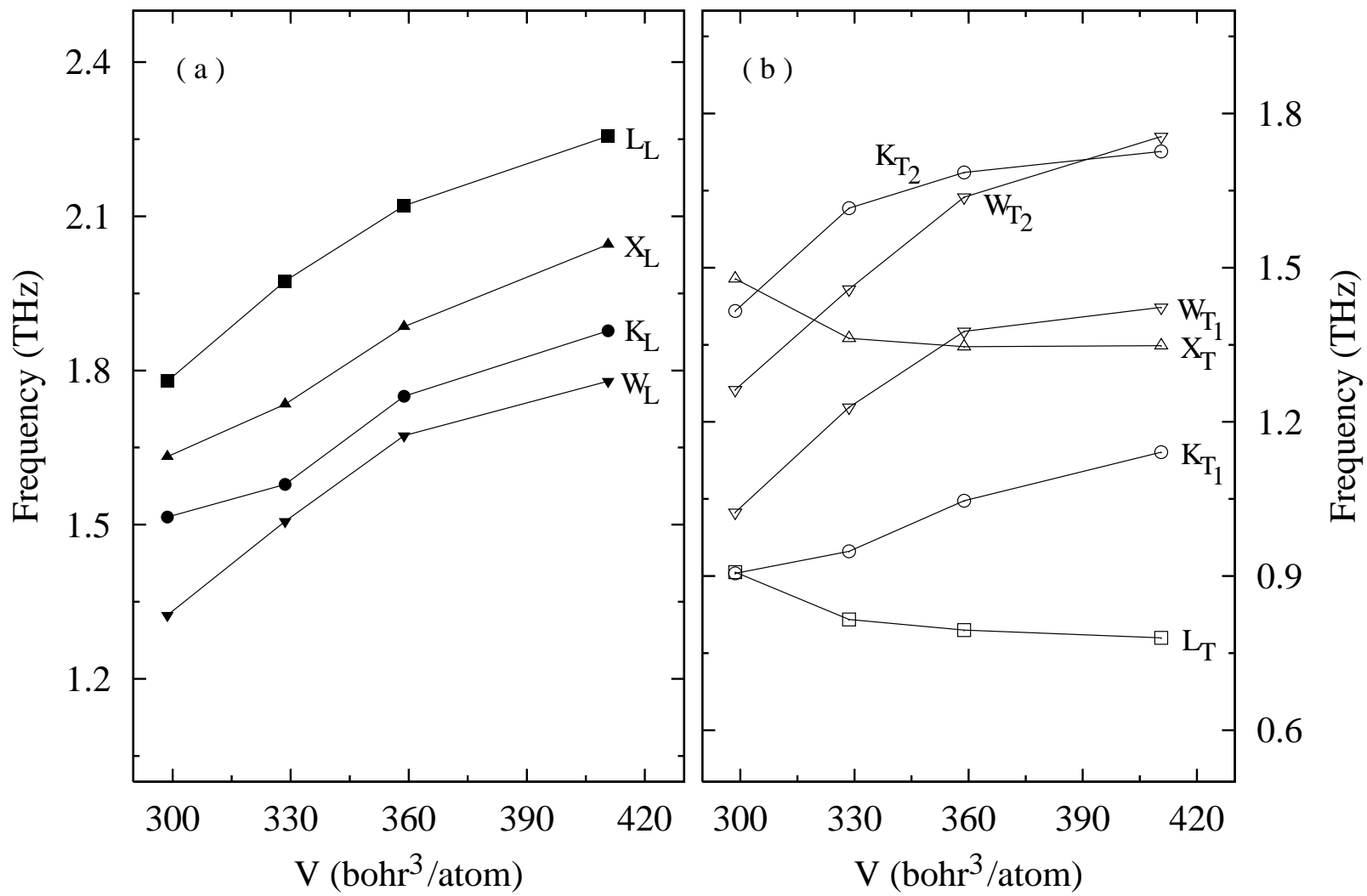


Fig. 2 of Y. Kong et al.

Fig. 3 of Y. Kong et al.



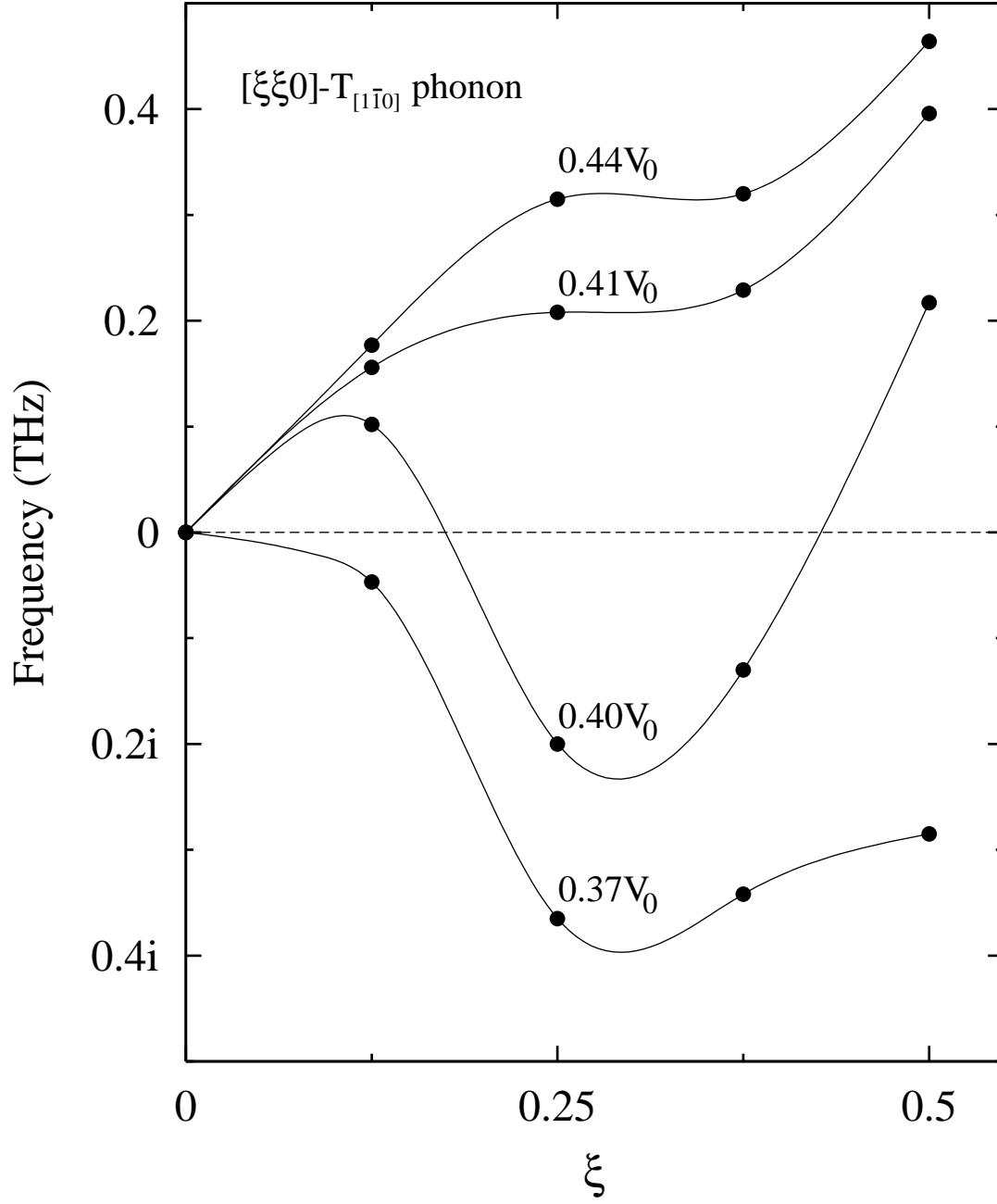


Fig. 4 of Y. Kong et al.

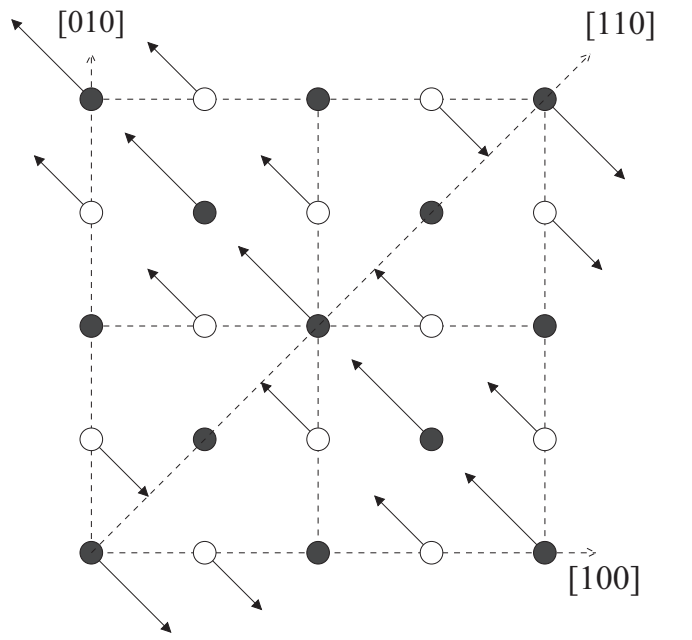
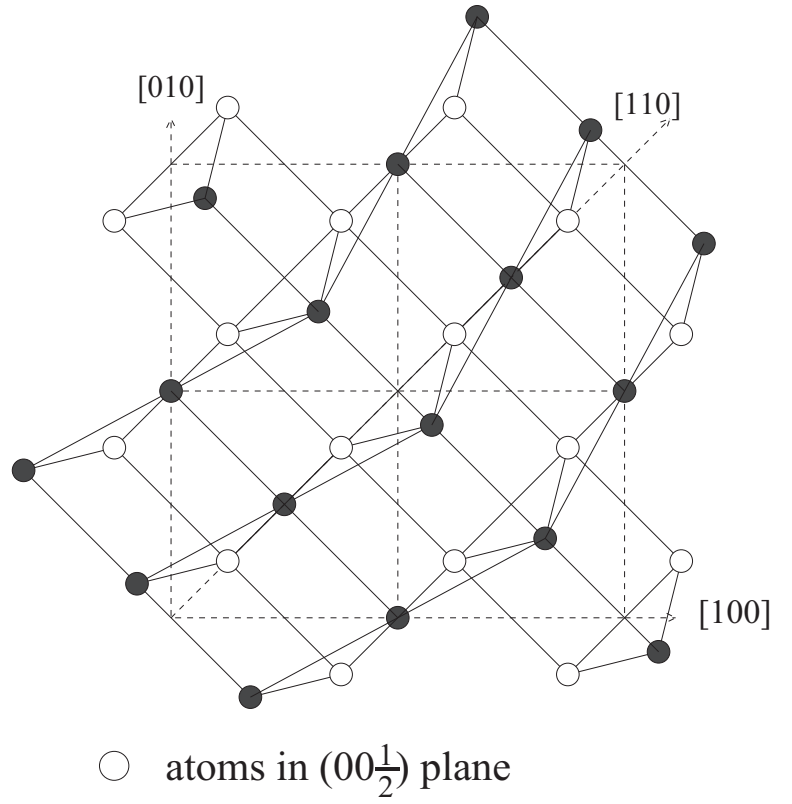


Fig. 5 of Y. Kong et al.